

The Finite Element Method with the Dirichlet-to-Neumann Map for Sound-Hard Rectangular Rooms

Yusuke Naka¹, Assad A. Oberai¹, Barbara G. Shinn-Cunningham²

¹Department of Aerospace and Mechanical Engineering

²Hearing Research Center

Boston University, Boston, MA 02215, USA

{ynaka, oberai, shinn}@bu.edu

Abstract

In this paper, the finite element method (FEM) is used to solve the Helmholtz equation for a rectangular room with sound-hard boundaries. An imaginary surface is introduced to truncate the room, reducing the effective room size and thus the computational costs. The boundary condition on the imaginary surface is the Dirichlet-to-Neumann (DtN) map that exactly models the effect of the portion of the room that is removed. Results suggest that in addition to the computational savings, introducing the imaginary boundary and using the DtN map yields more accurate results than the conventional FEM without a DtN map.

1. Introduction

Echoes and reverberation impact auditory perception in many ways, distorting auditory spatial cues, rendering speech less intelligible, and providing cues for source distance and room characteristics. In order to investigate the influence of room acoustics on perception (particularly spatial hearing), a realistic model of the impulse responses from a source to the left and right ears would be invaluable. However, many common methods for calculating such responses are based on geometrical approximations and simplifications that fail under certain conditions of interest to psychoacousticians, such as when the sound source is near the listener [1].

The finite element method (FEM) and the boundary element method (BEM) are useful in this context since they can account for relevant physical phenomena, such as diffraction, even in complex geometries [2]. Each of these methods has its own advantages and disadvantages. In the BEM, only the boundaries need to be discretized, and thus the size of the stiffness matrix, which consists of the coefficients of the unknowns, is small. It is, however, a dense matrix. In contrast, the FEM requires the discretization of the whole computational domain, and hence the stiffness matrix is large. However, it is sparse and as a result easier to solve.

Solving the FEM becomes computationally pro-

hibitive when applied to the acoustic problem inside a room with typical dimensions, because the size of the resulting stiffness matrix is large. In this work, we reduce the size of the stiffness matrix by truncating the domain at an imaginary surface and imposing the appropriate DtN map [3] boundary condition on the new, imaginary surface. Thereby it becomes feasible to use the FEM for solving this problem.

2. Problem description

The approach detailed below solves the scalar Helmholtz equation in rectangular-shaped rooms having sound-hard boundaries. The approach is also extended to the case in which the room contains sound-hard objects with irregular shapes.

2.1. General interior Helmholtz problem

Let Ω denote a closed domain and Γ denote its boundary. Formulated in this way, Γ includes all the walls of the room and the surfaces of the objects. If Γ is sound hard, then the problem for the acoustic pressure p can be solved by finding p such that:

$$-\nabla^2 p - k^2 p = g \quad \text{in } \Omega, \quad (1)$$

$$\nabla p \cdot \mathbf{n} = 0 \quad \text{on } \Gamma, \quad (2)$$

where $k = \omega/c$ is the wave number, ω is the angular frequency, c is the speed of sound, g is the forcing function, and \mathbf{n} is the outward unit normal vector on Γ . Note that (1) and (2) are the equations describing not only pressure p but other acoustic quantities such as density and particle velocity.

2.2. Interior Helmholtz problem with DtN map

2.2.1. Truncation of domain

We introduce an imaginary surface Γ_{dtN} that divides the domain Ω into two separate parts denoted by Ω_n and Ω_a . The problem is solved numerically in Ω_n and analytically in Ω_a . Objects with sound-hard boundaries can be placed

inside Ω_n , but not in Ω_a . For the computational domain Ω_n , the problem for the acoustic pressure p can be solved by finding p such that:

$$-\nabla^2 p - k^2 p = g \quad \text{in } \Omega_n, \quad (3)$$

$$\nabla p \cdot \mathbf{n} = 0 \quad \text{on } \Gamma_n, \quad (4)$$

$$\nabla p \cdot \mathbf{n} = M_{dtn}(p) \quad \text{on } \Gamma_{dtn}, \quad (5)$$

where $M_{dtn}(p)$ is the boundary condition imposed on Γ_{dtn} that exactly models the effect of the other portion of the overall domain, Ω_a . The boundary condition $M_{dtn}(p)$ is called the Dirichlet-to-Neumann (DtN) map.

The DtN approach has been applied to other problems in other domains (e.g., see [4]). Following these approaches, we find that the DtN map for a three dimensional room in the Cartesian coordinate system described in Fig. 1 is given by

$$M_{dtn}(p) = \sum_{m=0}^{\infty} \sum_{n=0}^{\infty} \alpha_{mn} \tan[\alpha_{mn}(L_x - x_{dtn})] \frac{\epsilon_m \epsilon_n}{L_y L_z} \times \int_{\Gamma_{dtn}} p(x_{dtn}, y', z') \cos\left(\frac{m\pi y'}{L_y}\right) \cos\left(\frac{n\pi z'}{L_z}\right) d\Gamma' \times \cos\left(\frac{m\pi y}{L_y}\right) \cos\left(\frac{n\pi z}{L_z}\right), \quad (6)$$

where

$$\alpha_{mn} = \sqrt{k^2 - \left(\frac{m\pi}{L_y}\right)^2 - \left(\frac{n\pi}{L_z}\right)^2}, \quad (7)$$

and ϵ_m is the Neumann factor having the value $\epsilon_m = 1$ if $m = 0$ but $\epsilon_m = 2$ if $m \geq 1$. Note that the DtN map for the two dimensional case can be obtained directly from (6) by simply setting $n = 0$ and $L_z = 1$.

2.2.2. FEM approach

The FEM is actually solved by finding the approximate solution to the equivalent weak form of (3) – (5). The

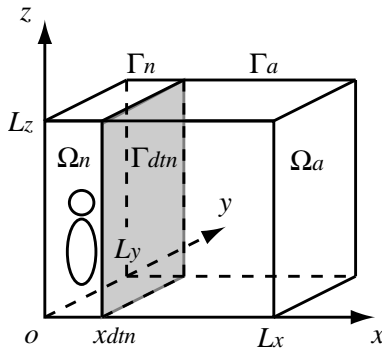


Figure 1: Coordinate system.

weak form associated with the DtN formulation is solved by finding $p \in \mathcal{S}$ such that $\forall w \in \mathcal{V}$:

$$a(w, p) - (w, M_{dtn}(p))_{\Gamma_{dtn}} = (w, g), \quad (8)$$

where

$$a(w, p) = (\nabla w, \nabla p) - k^2 (w, p). \quad (9)$$

The inner products (\cdot, \cdot) and $(\cdot, \cdot)_{\Gamma_{dtn}}$ used in (8) and (9) are defined by

$$(w, p) = \int_{\Omega_n} w p \, d\Omega, \quad (10)$$

$$(w, p)_{\Gamma_{dtn}} = \int_{\Gamma_{dtn}} w p \, d\Gamma. \quad (11)$$

Since all the boundaries are sound hard, the function spaces \mathcal{S} and \mathcal{V} are the same and defined as

$$\mathcal{S} = \mathcal{V} = \{v \mid v \in H^1(\Omega_n)\}. \quad (12)$$

3. Implementation

To solve the problem by the Galerkin FEM, we use the QMR method together with the SSOR preconditioner [5]. The QMR method, like other Krylov-subspace iterative methods [5], requires the computation of matrix-vector products at each iteration. Most of the computational effort required to solve the current problem is devoted to calculating these matrix-vector products. The matrix multiplied by the vector (the stiffness matrix) can be represented as a sum of two matrices, one associated with the computational domain Ω_n and one that reflects the contribution of the DtN boundary condition. The former matrix is sparse, while the latter is dense. Effective algorithms to reduce the computational penalty of the matrix-vector product associated with the dense part of the stiffness matrix [6] are used to manage the computational effort.

4. Results

This section shows computational results for two three-dimensional examples using the DtN map. In the first example, the accuracy and efficiency of the DtN computational solution are compared to both the analytic solution and the solution found using the pure FEM computational approach. The second example explores how the DtN and pure FEM solutions are influenced by objects inside Ω_n .

In both examples, a rectangular room with sound-hard boundaries is considered. The dimensions of the room are $L_x = 2.8\text{m}$, $L_y = 2.2\text{m}$, $L_z = 2.4\text{m}$, $x_{dtn} = 0.5\text{m}$ (see Fig. 1). The receiver position is $\mathbf{x}_r = (0.4, 1.6, 2.0)$ and the point source, which is chosen as the forcing function, is placed at $\mathbf{x}_s = (0.3, 0.3, 1.0)$. The numeric computations are halted when the residual drops to less than 10^{-5} of the initial residual. M_{dtn} is approximated using the first eleven modes in each of y - and z -directions (i.e., summing (6) over $0 \leq m, n \leq 10$) when

the wave number k is less than or equal to 10.0. If k is greater than 10.0, the number of modes used to approximate M_{dtn} is set by adding one to the integer portion of the wave number.

4.1. Example 1: Room without objects

Analytical, pure FEM, and FEM with the DtN solutions are first found for the room when it is empty. Table 1 shows the computational time and the numbers of iterations needed for convergence of the pure FEM and the FEM with the DtN map at $k = 10.0$, which corresponds to 509.3 Hz. The time per iteration, also shown in Table 1, is estimated by dividing the total computational time by the number of iterations.

Table 1 shows that the time for each iteration is reduced by including the DtN map (as expected given that the size of the stiffness matrix is reduced). Moreover, the number of iterations required for convergence is greatly reduced. As a consequence, the total computational time of the DtN method is reduced by 88 percent relative to the time required for the traditional FEM approach. The introduction of the DtN map drastically improves the efficiency.

Fig. 2 shows the analytic solution, the full FEM numerical solution, and the numerical solution for the FEM with the DtN map as a function of frequency. Note that the result for the non-DtN case is obtained only up to $k = 12.0$ since it is not feasible to perform the computation for higher frequencies. For each frequency f , the normalized error at the receiver position, $e(f)$, is found as

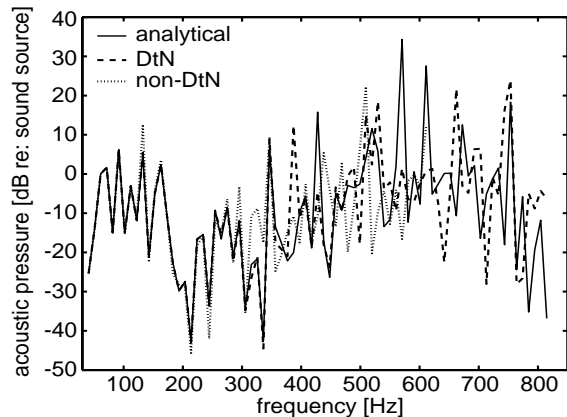
$$e(f) = \frac{|p(f) - p_{exact}(f)|}{|p_{exact}(f)|}, \quad (13)$$

where $p(f)$ and $p_{exact}(f)$ are the numerical and analytical solutions, respectively.

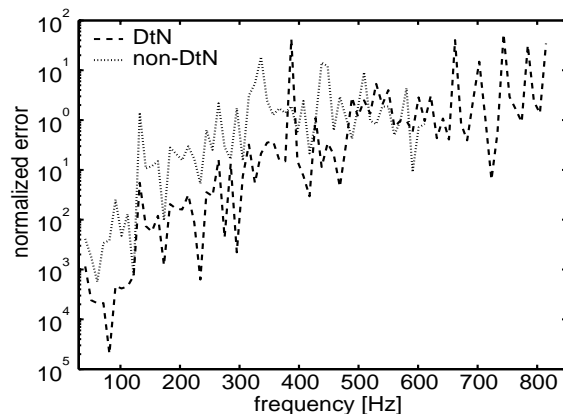
Fig. 2 (b) shows $e(f)$ for the FEM solutions with the DtN map and without the DtN map. Results show that the errors in both the DtN and the non-DtN cases grow as the frequency increases, a well-known result of the Galerkin finite element method [7]. However, more importantly, the DtN map solution gives more accurate results than the standard FEM. While important, this result is not surprising considering that the problem is solved analytically in Ω_a without any approximation. Therefore, the DtN map

Table 1: Computational costs.

example (wave number)	method	time (min)	iterations	time per iteration (sec)
1 ($k = 10.0$)	DtN	43	2311	1.1
	non-DtN	358	9448	2.3
2 ($k = 5.0$)	DtN	11	550	1.3
	non-DtN	70	1871	2.2



(a) Numerical and analytical solutions.



(b) Error in numerical approaches

Figure 2: Solutions at $\mathbf{x}_r = (0.4, 1.6, 2.0)$ and $\mathbf{x}_s = (0.3, 0.3, 1.0)$ in an empty, rectangular room.

solution contains the exact effect of Ω_a and results are more accurate with the DtN map as long as M_{dtn} is found with sufficient accuracy (i.e., including enough modes).

4.2. Example 2: Room with objects

In the second example the same room is considered, but a simple model of the KEMAR mannequin with sound-hard surfaces is modeled in Ω_n [8]. The head and the torso are modeled as a sphere and an ellipsoid respectively. The center of the sphere is at $(0.3, 0.4, 1.0)$ and the back side of the model is facing the plane $x = 0$. The same source and receiver positions are used as in the results shown in Fig. 2. The sound source is located at the entrance of the external ear canal so that, eventually, we can use the reciprocity principle to efficiently obtain the reverberant head-related transfer function (HRTF) or the binaural room impulse response (BRIR) [8].

Fig. 3 shows the results for the computation with and without the DtN map. Each panel gives the contour plot of the solution on the vertical plane containing the center of the sphere and the source position for wave number

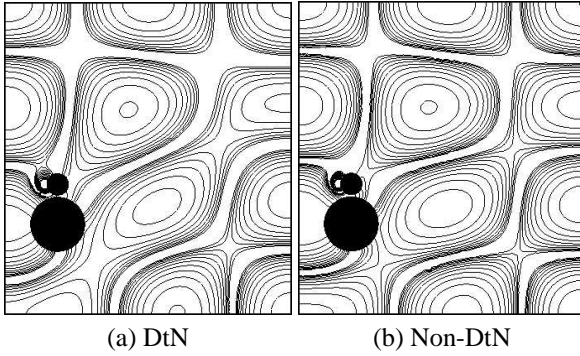


Figure 3: Contour plot of pressure in every 2 dB on the plane $x = 0.3$.

5.0. Panels (a) and (b) are almost identical, demonstrating that the DtN map can be used to truncate the computational domain and reduce computational complexity without loss of accuracy, even when there are objects within Ω_n .

The bottom entries in Table 1 show that the total computation time, the number of iterations, and the time per iteration are smaller with the DtN map than without. The time required for each iteration is almost the same as in Example 1 and the total computational time of the DtN method is about 16 percent of the non-DtN case. These results suggest that the improvement in computational efficiency afforded by the DtN is unaffected by the presence of the objects in the solution domain.

5. Conclusions and future work

In order to reduce the computational cost of solving a Helmholtz problem in a rectangular-shaped, sound-hard room using the FEM, the domain can be truncated by an imaginary surface on which the appropriate DtN boundary condition is imposed. Examples show that the introduction of the DtN map reduces the computational demands as expected. Moreover, the DtN approach gives more accurate results than the standard FEM.

While results are promising, the method is still limited in both the frequency range and the size of the domain Ω_n to which it can be applied. In order to be useful for finding BRIRs, both efficiency and accuracy must be further improved. Computational speed may be increased by introducing more than one imaginary surface, so that the computational domain is even smaller, or by the use of an FFT algorithm to reduce the computational costs of solving the matrix equation associated with the DtN map formulation. Similarly, there are several ways to improve accuracy. For instance, the Galerkin least square method is more accurate than the standard Galerkin method. We can also obtain more accurate solutions by using higher-order elements. Ultimately, such improvements may lead to a tractable numerical approach

for finding BRIRs in complex, reverberant listening environments directly from the solution to the Helmholtz equations.

6. Acknowledgments

This work was supported by grants from the Air Force Office of Scientific Research and the Alfred P. Sloan Foundation.

7. References

- [1] B. G. Shinn-Cunningham, J. G. Desloge, and N. Kopco, "Empirical and Modeled Acoustic Transfer Functions in a Simple Room: Effects of Distance and Direction," in *Proc. IEEE WASPAA*, 2001, pp. 183-186.
- [2] S. Kopuz and N. Lalor, "Analysis of Interior Acoustic Fields Using the Finite Element Method and the Boundary Element Method," *Appl. Acoust.*, vol. 45, pp. 193-210, 1995.
- [3] J. B. Keller and D. Givoli, "Exact Non-reflecting Boundary Conditions," *J. Comp. Phys.*, vol. 82, pp. 172-192, May 1989.
- [4] D. Givoli, I. Patlashenko, and J. B. Keller, "High-Order Boundary Conditions and Finite Elements for Infinite Domains," *Computer Meth. Appl. Mech. and Eng.*, vol. 143 (1-2), pp. 13-39, 1997.
- [5] Y. Saad, *Iterative Methods for Sparse Linear Systems*. Boston: PWS Publishing Company, 1995.
- [6] A. A. Oberai, M. Malhotra, and P. M. Pinsky, "On the Implementation of the Dirichlet-to-Neumann Radiation Condition for Iterative Solution of the Helmholtz Equation," *Appl. Numer. Math.*, vol. 27, pp. 443-464, 1998.
- [7] R. Mullen and T. Belytschko, "Dispersion Analysis of Finite Element Semidiscretizations of the Two-Dimensional Wave Equation," *Int. J. Numer. Meth. Eng.*, vol. 18, pp. 11-29, 1982.
- [8] V. R. Algazi, R. O. Duda, R. Duraiswami, N. A. Gumerov, and Z. Tang, "Approximating the Head-Related Transfer Function Using Simple Geometric Models of the Head and Torso," *J. Acoust. Soc. Am.*, vol. 112 (5), pp. 2053-2064, Nov. 2002.